12^{th} International Conference on Fracture Mechanics of Concrete and Concrete Structures
FraMCoS-12
B.L.A. Pichler, Ch. Hellmich, P. Preinstorfer (Eds)

https://doi.org/10.21012/FC12.1121
MS03-2:4

FRACTAL MICRO-CRACKING FEATURES IN CONCRETE UNDER FATIGUE AND MONOTONIC LOADING

ARKA MANDAL[*†] and J.M. CHANDRA KISHEN[*‡]

[*] Indian Institute of Science
Bengaluru 560012, India
[†] e-mail: arkamandal@iisc.ac.in
[‡] e-mail: chandrak@iisc.ac.in

Key words: Fractal Dimension, Concrete Fatigue, Acoustic Emission, Micro-crack coalescence

Abstract. The fracture process in concrete is a collaborative process among the micro-cracks originating ahead of the crack tip under the applied load, and influenced by the constituent heterogeneity. To understand this interactive phenomenon, statistical physics-based theories are very applicable, and by treating each micro-crack as an energy source, the whole process can be remodeled into a phase space. This study aims to investigate the sparsity of micro-cracking in concrete subjected to fatigue and monotonic loadings by utilizing the fractal signatures of the phase space constructed from the acoustic emission parameters. The correlation dimension of the acoustic emission energy time series generated from concrete for both types of loading is obtained separately using the Grasserberger-Proccacia algorithm. The results indicate that concrete under fatigue has a lower correlation dimension than the monotonic case, explaining that fatigue is a process where one crack causes failure, unlike the monotonic case, where it is a cooperative phenomenon. The correlation dimension can also capture the influence of cycling frequency on the fatigue life, showing an increment with the increase in frequency. The efficiency of this method can be enhanced by choosing the appropriate dimension of the underlying phase space of the time series and, therefore, can preferably employed to estimate the health of a real-life structure over conventional methods like event source localization.

1 INTRODUCTION

On a material level, concrete is heterogeneous, and it is not only due to the wide variety of ingredients in its mixture design, but also due to the presence of the unavoidable flaws like voids, pores and micro-cracks. When subjected to load, several other micro-cracks form ahead of the crack tip [1], and it is the inherent heterogeneity that do not allow them to localize and propagate easily [2] through several resistive processes known as the toughening mechanisms [3]. This forms a cloud of micro-cracks in front of the crack tip known as the fracture process zone (FPZ) and it is the FPZ which increases the resilience of the material, that is evident from the post-peak softening behavior in the tensile response of concrete [4]. Due to the toughening mechanisms such as crack branching and crack deflection [5], the most probable method to cause global failure is to form a macro-crack by the coalescence of several micro-cracks, thus making concrete fracture an interactive phenomenon. Therefore, it is very important to develop an in depth understanding of the material behavior, in order to utilize

the post-peak response to the fullest while designing real life structures. To achieve this, the material must be monitored from within and that too in real time, hence acoustic emission (AE) sensing technique is preferred [6], and as concrete exhibits a pronounced softening response, adequate number of AE signals are received prior to the complete failure [7]. All these traits allows concrete to be classified as a quasi-brittle material. However, these properties are dependent upon the size of the specimen [2] and also upon the nature of the sustained loading, because failure of concrete is an interplay between the heterogeneity and the applied load. Hence, the influence of the applied loading is very important [8] in the context of the softening response and the precursory AE signals.

For this study, the effect of fatigue loading on the formation of a cloud of micro-cracks ahead of the crack tip, similar to what occurs under conventional monotonic loading is examined. The main reason to investigate the influence of fatigue, apart from it being cyclic in nature is the fact that, it causes sub-critical failure. The softening behavior of concrete is observed only when the peak strength or the critical load is exceeded, but the sub-critical failure due to fatigue happens suddenly and that too before reaching the peak load, which makes it an extremely severe class of loading. In fact, creep is also a sub-critical type of failure, but is not as severe as fatigue, because the former takes a significantly longer duration and exhibit enough visual indicators before failure, unlike fatigue [9]. Some studies have been carried out using AE in order to look into the micro-cracking features of concrete fracture under fatigue, and it was reported that the micro-cracking density is significantly low as compared to that under monotonic loading [10]. Considering the principal attribute of concrete fracture, that is the interaction among micro-cracks, fundamental principles of statistical physics are the most suitable [11, 12] to look into the process in a greater detail.

Usually to study the development of the FPZ, the position of the micro-cracks are precisely obtained from AE localization techniques, but this method is very time consuming [13]. Considering the very first aspect of statistical physics, namely the interactions within a many bodies system [14], where the energy of the system depends upon the position vectors of the individual bodies, a phase space is constructed in order to give a geometric representation of the mechanical state of the system.

Utilizing the fractal nature of the micro-crack positions and dimensions inside the FPZ [15], and the power-law distribution of AE energy time series, an equivalent phase space is constructed from the AE energies to study the sparsity of micro-cracking within notched concrete beams under three point bending due to fatigue and monotonic loadings respectively. Apart from the theoretical considerations one practical motivation is that, this method is fairly applicable even when events are not captured, as multiple number of sensors are required to get the locations, but the AE energies can be obtained from one sensor as well.

2 METHODOLOGY

It is now understood that the fracture process of concrete is a collective phenomenon [11], which at any point of time is dependent upon the concentration of the micro-cracks formed within the material [2] and their mutual interactions. Therefore, in order to study the fracturing phenomenon, precise temporal and spatial description of the material bulk is required, which is successfully obtained with the aid of AE, but the computational cost of the process of source localization is very high [13]. In order to overcome this limitation, theories that specialize in many body interactions are required, and most of such theories have their

core within the field of statistical physics [7]. The state of any mechanical system is determined from the spatial coordinates that may or may not change with respect to time [14]. However, these systems can also be uniquely and accurately characterized using other features as well that evolve with time and the new describing coordinate system formed is known as the phase space. In the phase space, at any time instant, the mechanical state is represented using a single point and the evolution of the system is automatically obtained from the trajectory of the point. Since the trajectory is a geometric feature, concept of fractality can be used to describe it. In fact, this procedure is used in an engineering sense in the area of structural dynamics [16] to study multi-degree of freedom systems.

In the present context, micro-cracks formed during the fracture process are treated as the quantities of interest and the phase space is constructed using the AE energies obtained from micro-cracks, and its fractal dimension is shown to be equivalent to that of the space obtained from actual event source localization [13].

It is known very fairly that the position of the micro-crack centroids are fractal in nature with respect to the specimen size s, and the fractality is measured in terms of a coefficient known as the correlation dimension D, which is a type of fractal dimension. The expression of this fractal distribution of given as [13]:

$$N(s) \sim s^D \tag{1}$$

where, $N(s)$ is the number of micro-cracks in a specimen whose largest geometric dimension is s. Now, using the ball covering method to calculate the fractal dimension, the following power-law type relation is obtained:

$$N(d) \sim d^{-D} \tag{2}$$

with d as the radius of the ball and $N(d)$ is the number of balls of radius d required to cover the entire crack network. This inverse power-law relationship can be explained from the Figure 1. When the radius is d the number of balls required are four, and once the radius of the covering balls are halved as in Figure 1b, the number of balls required to cover the same area is squared to sixteen.

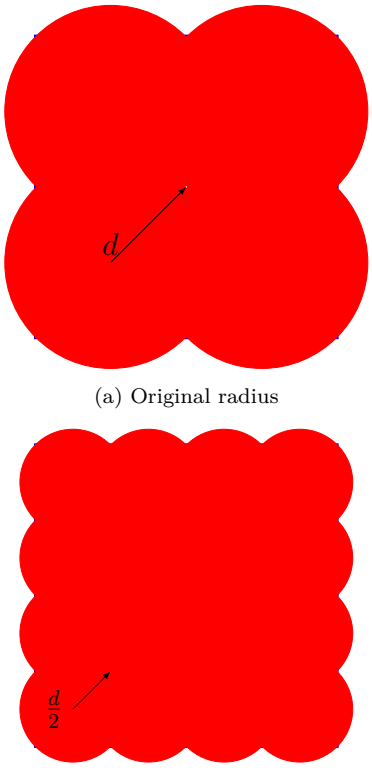

(a) Original radius

(b) Radius halved

Figure 1: Ball covering method

Now, combining Equation 1 with Equation 2 retrieves the original definition of fractals, which is:

$$N(d) \sim \left(\frac{s}{d}\right)^D \tag{3}$$

From the fractal theories of fragmentation and particle size distributions [15], the cumulative number of micro-cracks of linear size L is a power-law distribution with exponent γ [13] and is give as:

$$N(\geq L) \sim L^{-\gamma} \tag{4}$$

where, $N(\geq L)$ is the number of

micro-cracks with dimension greater than or equal to L. Assuming that the radius of the balls required is a power-law function of the linear dimension L with exponent x as:

$$d(L) \sim L^x \tag{5}$$

and due to the dependence of the radius d on the crack size L, Equation 3 is rewritten as:

$$N(\geq L) \sim \left(\frac{s}{d(L)}\right)^D \sim \left(\frac{s}{L^x}\right)^D \tag{6}$$

For a fixed specimen size s, the preceding equation is analogous to Equation 5, which gives the relationship between all the exponents [13] as:

$$x = \frac{\gamma}{D} \tag{7}$$

From the self-similar nature of micro-crack distribution within the FPZ [17], the exponent x relating the distance between two cracks of almost same size is a constant [13]. Therefore, making the power-law exponent γ proportional to the correlation dimension D as:

$$D \propto \gamma \tag{8}$$

Since the energies of the AE are directly proportional to the geometric dimension of the source, this means:

$$E \propto L \tag{9}$$

where E is the energy of an AE event. Thus from Equations 7 and 9 it is evident that measuring the fractal dimension of the physical event positions are equivalent to that of measuring the fractal dimension of the AE energy time series.

To find out the fractal dimension of a time series, the Grasserberger-Proccacia (GP) [18] algorithm shall be utilized. The procedure as follows. Considering a time series X as:

$$X = \{x_1, x_2, x_3, \cdots, x_n\} \tag{10}$$

The sequence given in Equation 10 containing n terms is embedded into a phase space of dimension m. To do so, the series in Equation 10 divided by sliding windows of size m, for example a two dimensional case is shown in Figure 2 for $m = 2$ and $n = 5$:

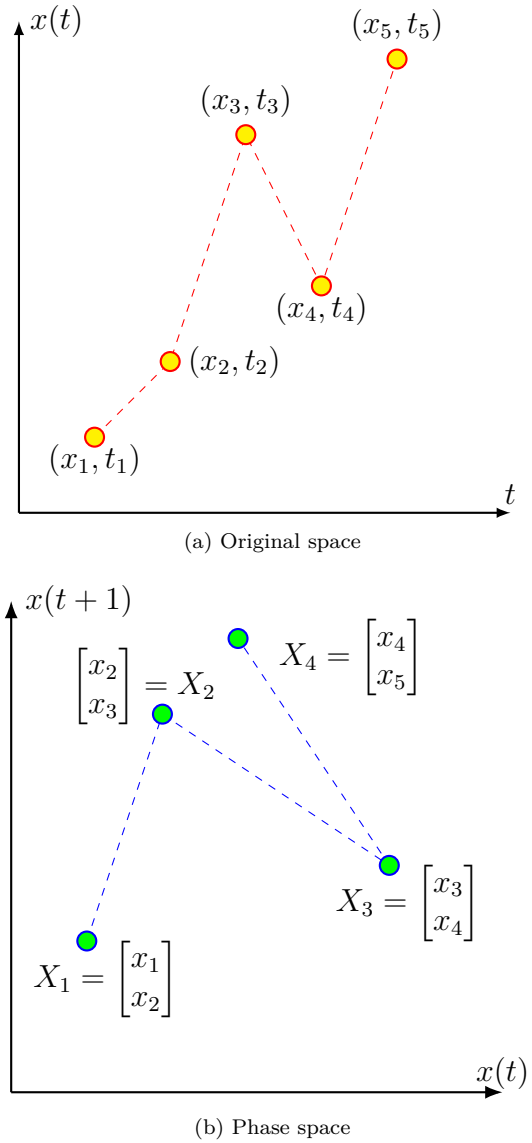

(a) Original space

(b) Phase space

Figure 2: Phase space construction

In general, for higher values of m, the vectors from Equation 10 are represented by taking the first m points, and then progressing by one vector each time as in Equation 11, producing a total of $n - m + 1$ vectors. The vectors $X_1, X_2, \ldots, X_{n-m+1}$ represent the points in the phase space.

$$X = \begin{cases} X_1 : (x_1, x_2, \cdots, x_m) \\ X_2 : (x_2, x_3, \cdots, x_{m+1}) \\ \vdots \\ X_{n-m+1} : (x_{n-m+1}, x_{n-m+2}, \cdots, x_n) \end{cases} \tag{11}$$

By reforming the time series in Equation 10 like Figure 2b and Equation 11, the correlation cumulative function $C(d)$ over ${}^nC_2 = \frac{n(n-1)}{2}$ micro-cracks is evaluated as [19]:

$$C(d) = \frac{2}{n(n-1)} \sum_{i=1}^{n-1} \sum_{j=i+1}^{n} \mathbb{H}\left(d - |X_i - X_j|\right) \tag{12}$$

where, $\mathbb{H}(u)$ is the Heavside step function, and is used to count the number of pairs of points, whose euclidean distance is less than or equal to d. It is defined as:

$$\mathbb{H}(u) = \begin{cases} 1, & u \geq 0 \\ 0, & u < 0 \end{cases} \tag{13}$$

Rewriting Equation 12 within proper range of d and m, for n number of cracks as a power-law:

$$C(d) \propto d^D \tag{14}$$

where, D is same as that in Equation 1 and the d is the representative of the hypothetical balls similar to that in Equation 2.

3 EXPERIMENTAL PROTOCOL

Notched plain concrete beams were prepared from a mixture of water, cement, fine aggregates and coarse aggregates, at a proportion of 1:0.54:1.08:1.62:1.62 and this resultant mixture produced cubes of dimension $150mm \times 150mm \times 150mm$, whose 28 days compressive strength were approximately $40MPa$ [20]. The mechanical tests were performed on a servo hydraulic universal testing machine of capacity $35kN$, manufactured by BISS (M/s ITW INDIA). The crack mouth opening displacement (CMOD) was measured through a clip gauge, whose working range was between $\pm 0.25mm$. The monotonic tests were performed with the CMOD as the control parameter at a rate of $10^{-3}mm/s$, while the constant amplitude cyclic tests were performed with the vertical actuator load as the control parameter at a fixed frequency. The in-plane geometry of the notched beams is shown in Figure 3. The supported length of the beams was $600mm$, the depth of the beam was $150mm$. The out-of plane thickness was set to be $50mm$ and the notch depth was fixed at $30mm$ for all the specimens.

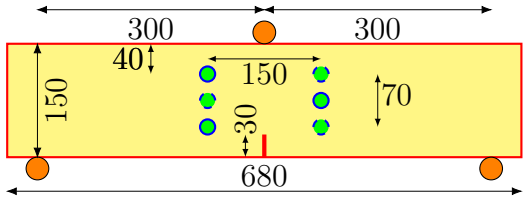

Figure 3: Specimen geometry with AE sensor positions (All dimensions are in mm)

Multiple specimens were tested for the monotonic case [20], out of which one representative test is shown in Figure 4 and the average peak strength was found out to be $3.35kN$.

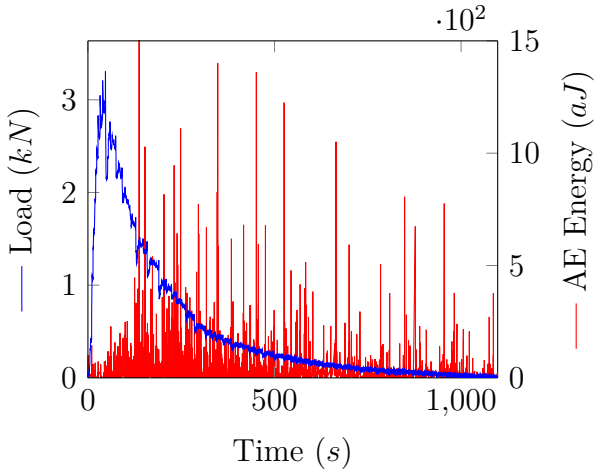

Figure 4: Monotonically loaded specimen

Figure 4 also shows in red the AE

energies emitted from within the specimen when loaded monotonically. These AE signals were captured using six $R6D$ type piezoelectric sensors, manufactured by MISTRAS Physical Acoustics, mounted on each surface with just adequate amount of silicon grease and later an outer plastic tape was wound in order to prevent the sensors from dislocating. The green filled blue circles in Figure 3 represent the sensors, with the dashed circles indicating the rear face of the beam and the rest are on the front.

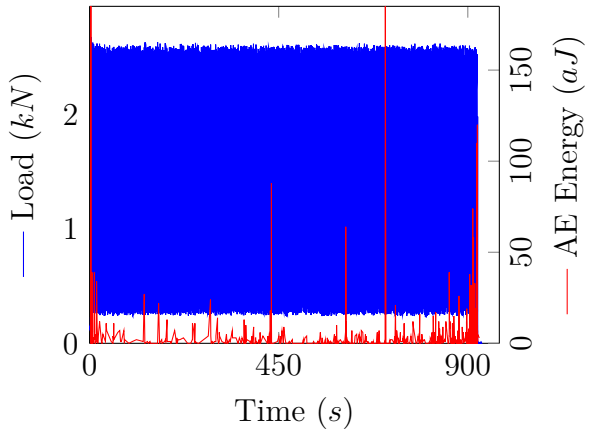

(a) $0.5Hz$ Fatigue test

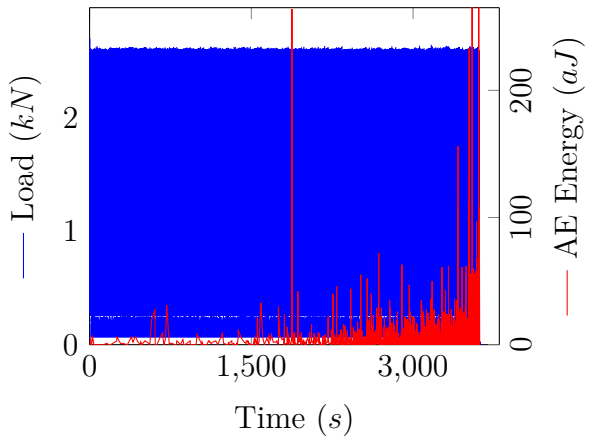

(b) $2Hz$ Fatigue test

Figure 5: Cyclically loaded specimens

For the fatigue loading, the specimens were sinusoidally cycled below their 80% of their static strength, which is expected to be $3.35kN$, and the lower limit was set at $0.25kN$. Effect of two cycling frequencies, namely $0.5Hz$ and $2Hz$ were studied on separate specimens. Even in these cases multiple specimens were tested, but only the representative cases, one of each are shown in Figure 5a and 5b.

Table 1: Summary of Experimental results [20]

Test type	CMOD^{max} (mm)	N_f $\otimes$	P_{max} (kN)
Monotonic	1.1	$\otimes$	3.35
$0.5Hz$ fatigue	0.08	1082	0.8×3.35
$2Hz$ fatigue	0.2	6861	0.8×3.35

Table 1 reports the mean values of important parameters such as, the maximum load (P_{max}) sustained by the specimen, the CMOD at failure ($CMOD^{max}$) and the number of cycles to failure when subjected to fatigue (N_f). Now, based on the AE energies captured by the sensors, a time series is constructed analogous to Equation 10 and the phase space is constructed in the form of Equation 11 by selecting an appropriate value of m.

4 RESULTS AND DISCUSSIONS

For the physical phase space constructed from the actual AE event locations, the value of m is fixed at 3.

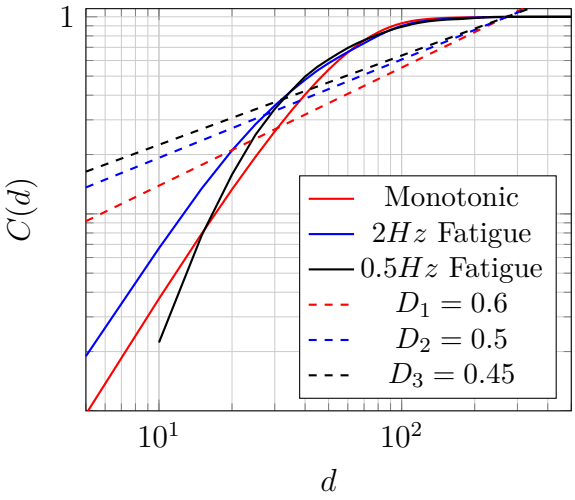

Figure 6: Correlation dimensions obtained from AE event locations

Using the GP algorithm, the correlation function as in Equation 12, is plotted in

Figure 6. Here the value of m cannot exceed 3, because the event positions are obtained in a three dimensional real euclidean space. In order to check the validity of the discussed method involving the AE energy time series, the value of m is selected to be 3 [19]. The correlation function of Equation 12 is shown in Figure 7.

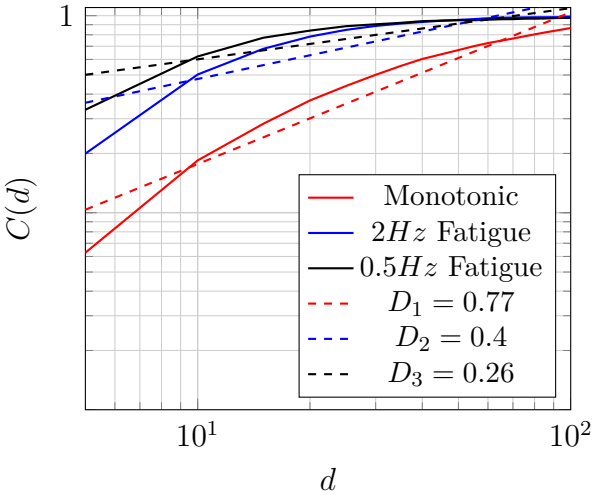

Figure 7: Correlation dimensions obtained from AE energy

Figures 6 and 7 reveal that the fractal dimension in the case monotonic (D_1), $2Hz$ fatigue loading (D_2) and at last the $0.5Hz$ fatigue loading (D_3) respectively follow the order:

$$D_1 > D_2 > D_3 \tag{15}$$

The increase in the fractal dimension for the monotonic case in the original physical space gets reflected in the alternate space constructed from the AE energy, justifying the relations obtained in Equations 8 and 9 respectively.

Although the results are quite convincing, the computational efficiency of the discussed method still remains the same, as the phase space dimension m is same for both the cases. To improve the efficiency, a larger value of m can be selected in order to reduce the number of vectors $X_1, X_2, \ldots, X_{n-m+1}$. Since the space constructed from the AE energies is not a physical space, there is no restriction on the value of m, and upon increasing the value of m the value of D usually increases as shown:

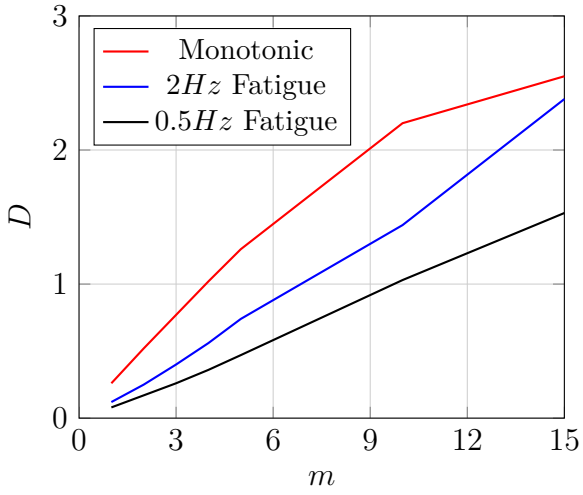

Figure 8: Plot of phase space dimension and fractal dimension

As shown in Figure 8, the fractal dimension for the monotonic case is the highest one and then are followed by the $2Hz$ fatigue specimen and then at last the $0.5Hz$ specimen, hence preserving the order of Equation 15 till values of m as large as 5 times the conventional value. Upon increasing the value of m, the number of vectors required to represent the time series in Equation 11 decreases, consequently reducing the compilation time. This shows that the fractal dimension is highest in the case of monotonic loading than those of the fatigue cases, even for large values of m. Also, it can be observed that with the increase in the cycling frequency, the correlation dimension increases.

From Figure 9, it can be seen that as the micro-crack coalescence represented by red dots progresses, number of balls required to cover them reduces, and from the definition in Equation 1, it is clear that the corresponding correlation dimension D also decreases. Therefore, it can be understood that the correlation dimension D of the AE time series is a very good estimator of the

micro-crack spreading ahead of the crack tip. Therefore, the increase in N_f and $CMOD^{max}$ with an increase in the cycling frequency can be attributed to the increase in D.

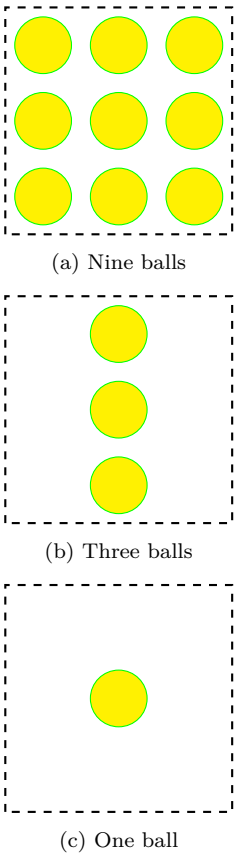

(a) Nine balls

(b) Three balls

(c) One ball

Figure 9: Reduction in fractal dimension with increasing micro-crack coalescence

A higher value of D indicates a higher density of micro-cracking, making the process a cooperative one, in contrast to a lower value, which represents a competitive process where a single crack causes the failure. These findings can be reinforced with the results obtained from actual AE event positions [10, 20] where it was reported that, under monotonic loading the micro-crackings were significantly more, as shown in Figure 10. This implies that the toughening mechanisms were more actively participating in the crack arresting process for the monotonic case and therefore results in a pronounced softening response, as shown in Figure 4. Whereas for fatigue, there was a drastic decrease in the number of micro-cracks, and thus justifying the fact that fatigue induced fracture is a sudden and abrupt incident. Similarly, with the increase in the cycling frequency, the event densities were relatively higher [21], which provides an account for the increase in the fatigue life cycles. The justification of Equation 15 can intuitively from the AE event locations in Figure 10.

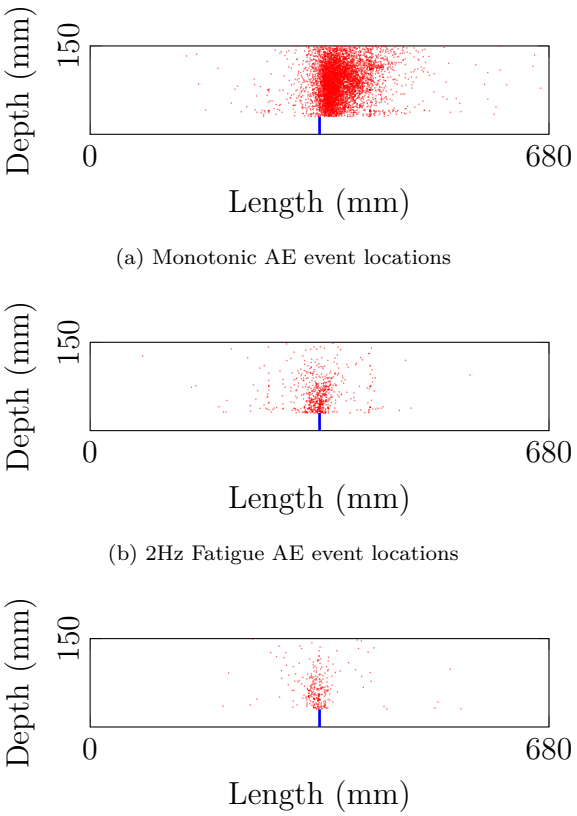

(a) Monotonic AE event locations

(b) 2Hz Fatigue AE event locations

(c) 0.5Hz Fatigue AE event locations

Figure 10: AE event locations

This justifies the fact that fatigue induced fracture is a competitive phenomenon rather than a cooperative one [22]. Under fatigue, an interesting observation is that with the increase in cycling frequency, the life cycles increase [20], and this can be attributed to the increment in D. In summary, for the monotonic case, more number of micro-cracks interact within the FPZ, in contrast to the case of fatigue, where the

influence of the process zone is negligible.

5 CONCLUSIONS

Based on the fact that the fractal dimension of the actual phase space constructed from the AE event locations is same as that of the one constructed from the AE energy time series, the following points can be concluded:

- The fractal dimension D is a direct measure of the micro-crack sparsity and density. Since, D is much higher for monotonically loaded specimen than that of the cyclically loaded specimens, it can be confirmed that monotonically loaded fracture is a cooperative process while fatigue induced fracture is competitive process and thus explaining the severity of fatigue over monotonic loading.
- With the increase in the cycling frequency, more number of micro-cracks are formed and thus there is a relatively higher proportion of toughening mechanisms take place, and this results in a higher CMOD^{max} and N_f values respectively.
- Even selecting a higher value of m successfully distinguishes between fatigue and monotonic fracture specimens based on the AE energies, but with a lower computational effort, as the number of constituting vectors $X_1, X_2, \ldots X_{n-m+1}$ reduces.
- Since this method does not require the event locations, lesser number of AE sensors can also be used for on site health monitoring. This method is much more computationally inexpensive as well, and can be further optimized by selecting higher values of m.

This method fetches satisfactory results with lesser number of AE sensors and also with lesser computational effort, actual large scale structures like dams and buildings [15] can be monitored in real time. In fact, this technique can be utilized to study the micro-crack initiation and macro-crack formation at the rock and concrete interfaces of dams, and as expected, the value of the fractal dimension reduces as the macro-crack progresses by consuming micro-cracks ahead of it, with the increase in the overload [23].

REFERENCES

[1] Jan G.M. van Mier. Framework for a generalized four-stage fracture model of cement-based materials. *Engineering Fracture Mechanics*, 75(18):5072–5086, December 2008.

[2] Zdenek P. Bažant, Jia-Liang Le, and Marco Salviato. *Quasibrittle Fracture Mechanics and Size Effect: A First Course*. Oxford University Press, Oxford, November 2021.

[3] S. P. Shah and C. Ouyang. Toughening mechanisms in quasi-brittle materials. *Journal of Engineering Materials and Technology*, 115(3):300–307, July 1993.

[4] Koji Otsuka and Hidehumi Date. Fracture process zone in concrete tension specimen. *Engineering Fracture Mechanics*, 65(2–3):111–131, January 2000.

[5] Victor C. Li and Mohamed Maalej. Toughening in cement based composites. part 1: Cement, mortar, and concrete. *Cement and Concrete Composites*, 18(4):223–237, 1996.

[6] Eric N. Landis. Micro–macro fracture relationships and acoustic emissions in concrete. *Construction and Building Materials*, 13(1–2):65–72, March 1999.

[7] Soumyajyoti Biswas, Purusattam Ray, and Bikas K. Chakrabarti. *Statistical Physics of Fracture, Breakdown, and*

Earthquake: Effects of Disorder and Heterogeneity. Wiley, May 2015.

[8] Jaap Weerheijm. *Understanding the Tensile Properties of Concrete*. Elsevier, 2024.

[9] Zdeněk P. Bažant and Yuyin Xiang. Crack growth and lifetime of concrete under long time loading. *Journal of Engineering Mechanics*, 123(4):350–358, April 1997.

[10] Radhika V. and J.M. Chandra Kishen. A comparative study of crack growth mechanisms in concrete through acoustic emission analysis: Monotonic versus fatigue loading. *Construction and Building Materials*, 432:136568, June 2024.

[11] Purusattam Ray. Statistical physics perspective of fracture in brittle and quasi-brittle materials. *Philosophical Transactions of the Royal Society A: Mathematical, Physical and Engineering Sciences*, 377(2136):20170396, November 2018.

[12] Mikko J Alava. How materials get tired. *Journal of Statistical Mechanics: Theory and Experiment*, 2007(04):N04001–N04001, April 2007.

[13] Alberto Carpinteri, Giuseppe Lacidogna, Gianni Niccolini, and Simone Puzzi. Morphological fractal dimension versus power-law exponent in the scaling of damaged media. *International Journal of Damage Mechanics*, 18(3):259–282, November 2008.

[14] Reinhold Haberlandt, Siegfried Fritzsche, and Horst-Ludger Vörtler. *Simulation of microporous systems: confined fluids in equilibrium and diffusion in zeolites*, page 357–443. Elsevier, 2001.

[15] Alberto Carpinteri, Giuseppe Lacidogna, and Simone Puzzi. From criticality to final collapse: Evolution of the "b-value" from 1.5 to 1.0. *Chaos, Solitons & Fractals*, 41(2):843–853, July 2009.

[16] Alberto Carpinteri and Nicola Pugno. Towards chaos in vibrating damaged structures—part i: Theory and period doubling cascade. *Journal of Applied Mechanics*, 72(4):511–518, April 2005.

[17] Jia-Liang Le, Zdeněk P. Bažant, and Martin Z. Bazant. Unified nano-mechanics based probabilistic theory of quasibrittle and brittle structures: I. strength, static crack growth, lifetime and scaling. *Journal of the Mechanics and Physics of Solids*, 59(7):1291–1321, July 2011.

[18] Miaoyan Liu, Jun Lu, Pan Ming, and Jia Song. Ae-based damage identification of concrete structures under monotonic and fatigue loading. *Construction and Building Materials*, 377:131112, May 2023.

[19] Kang Zhao, Qizheng Huang, Yun Zhou, Yajing Yan, Jian Yang, Chao Ma, Qiang Nie, Jiale Chen, and Yichen Shi. Fractal characteristics and acoustic emission b -value of cement superfine tailings backfill with initial defect consideration. *Nondestructive Testing and Evaluation*, 39(2):384–407, April 2023.

[20] K. Keerthana and J. M. Chandra Kishen. Micromechanical effects of loading frequency on fatigue fracture in concrete. *Journal of Engineering Mechanics*, 147(12), December 2021.

[21] K. Keerthana and J. M. Chandra Kishen. Effect of loading frequency on flexural fatigue behaviour of concrete. In *Proceedings of the 10th International Conference on Fracture Mechanics*

of Concrete and Concrete Structures, FraMCoS-X, France, June 2019. IA-FraMCoS.

[22] O Ostash. Fatigue process zone at notches. *International Journal of Fatigue*, 23(7):627–636, August 2001.

[23] Ying Zhang, Yaoru Liu, Zhuofu Tao, Haowen Zhou, and Qiang Yang. Fractal characteristics and failure analysis of geomechanical model for arch dam based on acoustic emission technique. *International Journal of Geomechanics*, 19(11), November 2019.